

# Interfacial Studies of Crosslinked Urethanes: Part III. Structure-Property Relationships in Polyester Waterborne Polyurethanes

M.W. Urban,\* C.L. Allison, C.C. Finch, and B.A. Tatro—North Dakota State University†

## INTRODUCTION

Polyurethanes (PURs) are high performance polymers known for their excellent properties among which such properties as abrasion resistance, hardness, flexibility, chemical and solvent resistance, gloss, low temperature film formation, and photolytic stability make them highly attractive for coatings applications.<sup>1-4</sup> Many properties are achieved by synthesis with numerous co-reactants,<sup>4-7</sup> making PURs a versatile class of polymers.<sup>1,8-13</sup> Due to increasing environmental concerns, waterborne (WB) PURs with equivalent properties to their solventborne counterparts appear to be of great importance. Although advantages of waterborne PURs are obvious, there are new challenges in synthesizing and formulating these polymers. The presence of water with relatively high surface tension creates difficulty in wetting substrates, and water may react with isocyanate, thus leading to property differences. Although the literature contains some information regarding WB PUR structure-property relationships,<sup>14,15</sup> in an effort to understand the factors that influence waterborne PUR film formation and structure-property relationships we initiated studies<sup>16,17</sup> on polyacrylate emulsions, which are extended to polyester dispersion polyurethanes. An ultimate goal of these studies is to compare the behavior of polyester dispersion and polyacrylate emulsion polyurethanes in terms of film formation near the film-air (F-A) and film-substrate (F-S) interfaces.

As was identified in our earlier studies,<sup>16</sup> the following moieties can be formed during PUR film formation: urethane, amine, carbon dioxide, and urea. Thus, we will examine crosslinking reactions and factors influencing waterborne polyurethane film formation near the F-A and F-S interfaces utilizing attenuated total reflectance Fourier-transform infrared (ATR FTIR) spectroscopy,<sup>17</sup> with focus on the formation of polyurethane/polyurea near the F-A and F-S interfaces.

*These studies examine crosslinking reactions of polyurethanes (PURs) using attenuated total reflectance Fourier-transform (ATR FTIR) spectroscopy and show that higher relative humidity (RH) accelerates the crosslinking reactions leading to the formation of polyurethane and polyurea. Concentration levels of unreacted isocyanate (NCO) are greater at the film-air (F-A) interface than the film-substrate (F-S) interface. In contrast to the previous studies on polyacrylate emulsion urethanes, no stratification was detected between 0.65 to 1.14  $\mu\text{m}$  near the F-A and F-S interfaces. This behavior is attributed to equivalent weight differences, 3100 g/eq for polyacrylate and 1140 g/eq for polyester. Solvent evaporation experiments show that approximately 10% of the initial water concentration remains in the film for extended periods of time, resulting in reactions leading to the formation of urea near the F-S interface. PUR film formation occurs in two stages, a solvent vapor pressure controlled stage, followed by a diffusion controlled stage. The duration of each stage depends on several factors, including the amount of shear induced on the shear thinning waterborne urethanes, which subsequently affects the exposure of isocyanate aggregates to water. Increased RH significantly affects structure-property relationships of waterborne PURs due to urea formation, which alters the glass transition temperature, storage modulus, crosslink density, and film hardness.*

\*To whom correspondence should be addressed.  
†Dept. of Polymers and Coatings, Fargo, ND 58105.

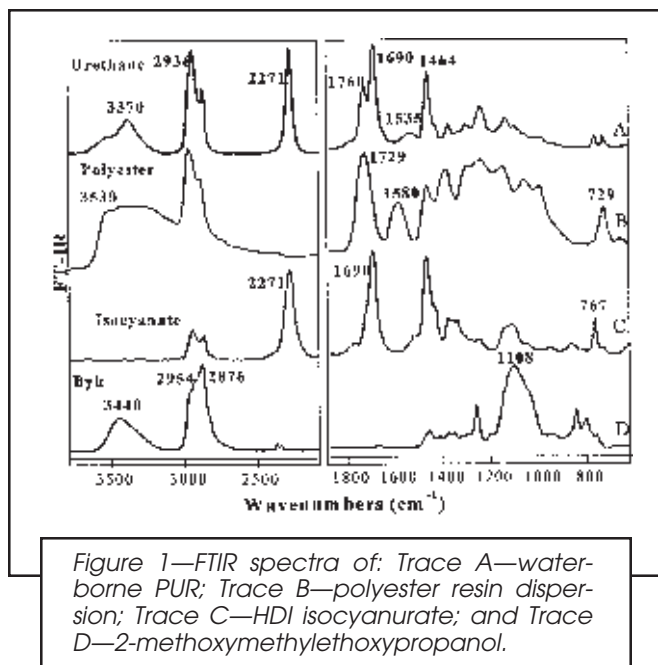


Figure 1—FTIR spectra of: Trace A—waterborne PUR; Trace B—polyester resin dispersion; Trace C—HDI isocyanurate; and Trace D—2-methoxymethylethoxypropanol.

## EXPERIMENTAL

### Sample Preparation

A polyester resin dispersion (XP-7093) and a hydrophilically modified aliphatic (HDI) polyisocyanate, 1,6-hexamethylene diisocyanate (NCO) (XP-7063), were supplied by the Bayer Corporation. Typical properties of XP-7093 resin are as follows: average acid number is 51, OH number is 49, and pH 7-8. An additive based on polyether modified dimethylpolysiloxane (BYK-346) was supplied by BYK Chemie. Two-component waterborne polyurethane was formulated at an NCO:OH equivalent ratio of 2:1. The polyester resin dispersion was mixed with the flow agent additive 2-methoxymethyl-

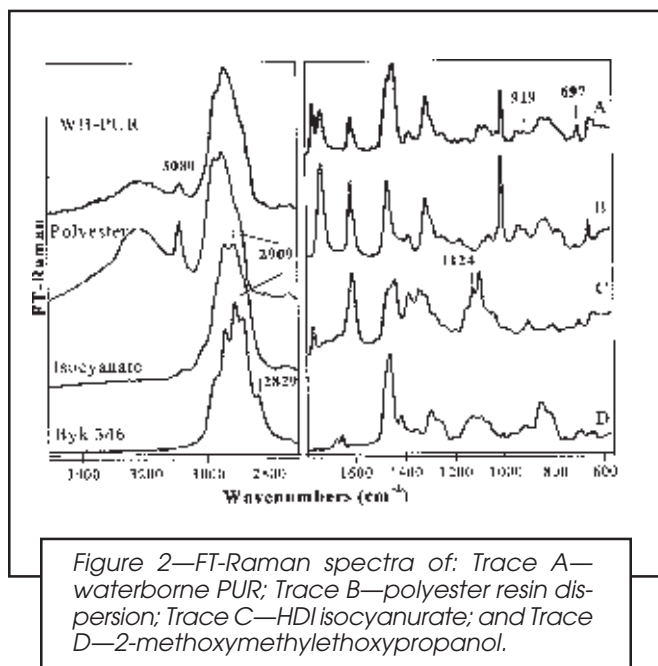


Figure 2—FT-Raman spectra of: Trace A—waterborne PUR; Trace B—polyester resin dispersion; Trace C—HDI isocyanurate; and Trace D—2-methoxymethylethoxypropanol.

ethoxypropanol (0.1 w/w%) at 48 rpm. Isocyanate and 2 mL of double deionized (DDI) water were added incrementally until a uniform dispersion, 150-300 cp, was obtained after seven minutes of mixing. The formulation was allowed to settle for five minutes before casting onto tin-plated steel panels at 75  $\mu\text{m}$  wet film thickness. The films were allowed to crosslink at 25°C under relative humidity conditions of 20, 40, 65, and 80%. Samples were removed periodically from the substrate for spectroscopic analysis using a mercury amalgamation method. An approximate dry film thickness was 19  $\mu\text{m} \pm 2 \mu\text{m}$ .

### Analytical Methods

Transmission, ATR, and Circle™ ATR FTIR were collected on a Nicolet Magna 850 spectrometer and purged with purified air (Whatman FTIR purge gas generator). The spectra were collected at 4  $\text{cm}^{-1}$  resolution using a 0.3165  $\text{cm/s}$  mirror speed. The ATR variable-angle multiple reflection attachment (Spectra Tech, Inc.) with 45° end cut parallelogram KRS-5 crystal was utilized. The depth of penetration was varied by changing the angles of incidence at 40, 45, and 60°, which correspond to 1.14, 0.92, and 0.65  $\mu\text{m}$  depths of penetration at 2271  $\text{cm}^{-1}$ . Polarized ATR FTIR spectra were collected with either parallel, transverse electric (TE; 0°), or perpendicular, transverse-magnetic (TM; 90°) polarized light using a Graseby Specac 12000 polarizer.

In a typical experiment, 60 co-added scans were ratioed against a background of 60 co-added scans of an empty ATR cell equipped with a KRS-5 crystal. ATR spectra of aqueous PUR were obtained by Circle™ ATR equipped with a ZnSe circular crystal at 45° (Spectra Tech Inc.). Liquid PUR was applied directly to the crystal, and the spectra were recorded as a function of time. Due to the fact that ATR spectra are a complex function of refractive index and absorption indexes, the dispersive nature of ATR spectra were corrected using Q-ATR software.<sup>18</sup> Corrected spectra were normalized to the  $\text{CH}_2$  stretching modes at 2936  $\text{cm}^{-1}$ . FT-Raman spectra were acquired on a Bruker Equinox 55 spectrometer equipped with a Bruker FRA 106 FT Raman accessory. The spectra represent 1000 co-added scans in a liquid cell, at 4  $\text{cm}^{-1}$  resolution using a 415 mW Nd:YAG laser excitation source. Spectral features of overlapping bands were deconvoluted with SS-RES maximum likelihood entropy method.<sup>19</sup>

Viscosity measurements were performed on a Carri-Med double concentric cylinder rheometer with a controlled stress of 2.657  $\text{sec}^{-1}$ . Measurements were taken at shear rates of 26, 48, 70, and 90 rpm. Conical mandrel flexibility (ASTM D 522)<sup>20</sup> (Sheen Instruments) was measured by bending the sample over a conical mandrel with the coating side on top. Specimens were bent until cracking occurs at the following intervals: 1, 3/4, 1/2, 1/4, and 1/8 in., where 1/8 in. is the most flexible. In the reverse impact resistance test (ASTM D 2794),<sup>20</sup> a 2.0 lb steel cylinder with a rounded head was dropped through a vertical shaft onto a coated steel panel, film side up. The maximum height at which this weight can be dropped without cracking the film is the impact strength (in.-lb). Knoop Tukon hardness (ASTM

**Table 1—Tentative FTIR and FT-Raman Band Assignments for Waterborne Polyester, HDI Isocyanurate, 2-Methoxymethylethoxypropanol, Polyurethane and Polyurea**

Band Assignment	Wavenumber (cm <sup>-1</sup> )							
	Waterborne Polyester		HDI Isocyanurate		2-methoxymethyl ethoxypropanol		Polyurethane	
	IR	Raman	IR	Raman	IR	Raman	IR	Raman
C-OH str. ....	3525				3440		3530	
N-H str. ....	3430						3377	
Overtone C=O .....	3214	3214						
v <sub>a</sub> C=C-CH <sub>2</sub> .....		3082						3080
v <sub>a</sub> CH <sub>3</sub> .....	2961	2967			2959	2966		2963
v <sub>a</sub> CH <sub>2</sub> .....		2945	2939	2937	2933	2936	2936	2936
R <sub>3</sub> C-H .....			2909		2904			
v <sub>s</sub> CH <sub>2</sub> .....	2890	2890	2864		2876	2876	28°63	2870
C-H str. aldehyde .....				Shoulder	2829,2731			
NCO out-of-phase .....			2271				2271	
Free C=O str. ....			1760	1762			1780	1760
Free C=O str. ....	1722	1729					1726	1729
H-bond. C=O str. ....			1691				1686	
C=O aldehyde .....					1658	1650		
C=C vinyl ether .....	1610	1613		1606			1610	1611
δ NH <sup>+</sup> 2 salt .....	1580	1594						
δ N-H & v <sub>a</sub> C-N amide II (urea) ....			1511				1535	
δ CH <sub>2</sub> .....	1464	1465	1465	1460	1455	1459	1464	1461
NCO in phase str. ....			1430	1435			1427	1442
C-H rock aldehyde .....					1415	1413		
δ-C(CH <sub>3</sub> ) .....	1386	1380	1374	1382	1375		1374	1374
δ N-H & v <sub>s</sub> C-N .....			1357		1352	1352		
NCO in-phase .....			1340	1336			1335	1330
CH <sub>2</sub> twist .....	1302	1312	1304	1314	1302	1293	1304	1307
(O=C)-O-C str. ....	1241	1248	1249	1241	1260	1264	1241	1245
v <sub>a</sub> C-N-C .....	1146		1143	1153				1156
C-C str. ....				1124		1124		
v <sub>a</sub> C-O-C .....		1083	1108	1099	1098	1126,1096	1097	1098
C-C skel. vib. ....	1055	1056	1048	1043			1058	1069
C-C-O out of phase .....	996	1008				1005	994	1006
C-C skel. vib. ....		943	952		954	968	942	942
C-C-O in phase .....		919		901		912		919
v <sub>s</sub> C-N-C .....			861	855			856	856
v <sub>s</sub> C-O-C .....	829	834	842	844	844	842	828	843
C-C-O in phase .....		775	767		757	757	766	776
CH <sub>2</sub> in-phase-rock .....	729		732				731	
v <sub>s</sub> C-C <sub>4</sub> .....		660		701,640		692,645		697,648
δ NCO .....			583					
δ C-O-C .....			431	438			428	438

v<sub>s</sub> = symmetric stretch  
v<sub>a</sub> = asymmetric stretch  
δ = deformation

D 1474)<sup>20</sup> was measured by a Tukon<sup>®</sup> Tester model MO, and the Knoop hardness number (KNH) was calculated by the following equation:<sup>20</sup>

$$\text{KNH} = \frac{L}{l^2 C_p} \quad (1)$$

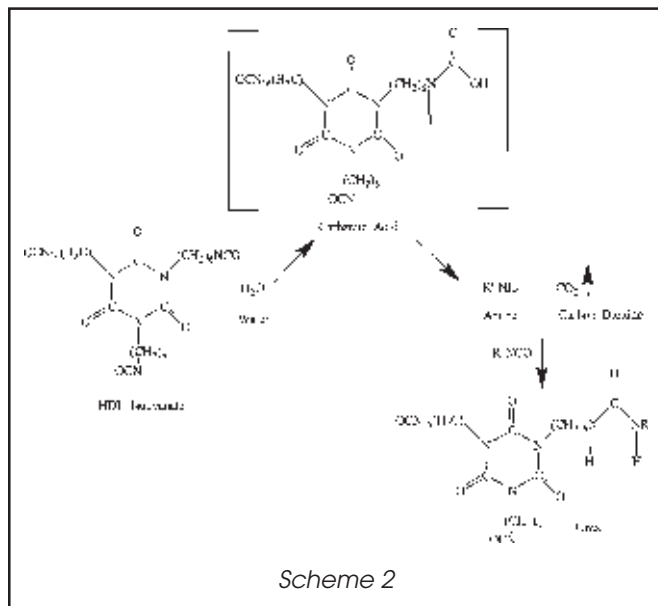
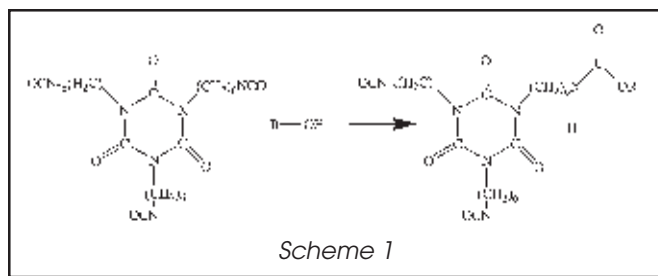
where L is the load applied to the indenter (0.025 kg), l is the length of the indentation (mm), C<sub>p</sub> is the indenter constant (7.028 × 10<sup>-2</sup>).

Dynamic mechanical thermal analysis (DMTA) was performed on a Rheometric Scientific DMTA 3E utilizing tension, compression geometry with a 6.2832 rad/sec frequency, 0.5% strain, autotension and a 5.0984 g initial static force. The samples were 5 mm × 9.5 mm and

0.02 mm thick, and measurements were taken from -100 to 250°C at 3°C/min.

## RESULTS AND DISCUSSION

The first step in this analysis will be to identify relevant spectral features responsible for PUR film formation. While Table 1 summarizes FTIR and FT-Raman active bands observed in individual urethane components and their tentative assignments, Figure 1 illustrates ATR and transmission FTIR spectra of waterborne polyurethane (Trace A), polyester resin dispersion (Trace B), HDI isocyanurate (Trace C), and 2-methoxymethylethoxypropanol (Trace D). The band at 2271 cm<sup>-1</sup> (Traces A and C)



is attributed to the out-of-phase stretching vibrations of NCO. This band is of particular interest because the NCO functionality dictates the crosslinking reactions of waterborne PURs. In the polyurethane spectrum (Trace A), the band at  $3370\text{ cm}^{-1}$  is due to N-H stretching vibration modes. The asymmetric  $\text{CH}_2$  stretching band at  $2936\text{ cm}^{-1}$  was used as the normalization band. Other  $\text{CH}_2$  deformation modes are detected at  $1466\text{ cm}^{-1}$ . The  $\text{C}=\text{O}$  stretching modes are detected at  $1760$  and  $1690\text{ cm}^{-1}$ , and are attributed to free  $\text{C}=\text{O}$  stretching vibrations and H-bonded  $\text{C}=\text{O}$  stretching vibrations of urea, respectively. Another band of interest is detected at  $1535\text{ cm}^{-1}$ , which is due to amide II stretching modes of polyurethane and polyurea. Figure 1, Trace B, shows the spectrum of polyester with the band at  $3530\text{ cm}^{-1}$  attributed to the OH functionality. The band at  $1729\text{ cm}^{-1}$  due to amide I stretching is present in the polyester dispersion and PUR spectra. The  $-\text{NH}_2^+$  salt deformation due to polyester dispersion is detected at  $1580\text{ cm}^{-1}$ . The  $\text{CH}_2$  in-phase rocking modes of the polyester at  $729\text{ cm}^{-1}$  also appear in the urethane spectrum. For reference, Trace D of Figure 1 illustrates an FTIR spectrum of 2-methoxymethylethoxypropanol, with the bands at  $2954$  and  $2873\text{ cm}^{-1}$  attributed to asymmetric and symmetric stretching modes of  $\text{CH}_3$  and  $\text{CH}_2$  groups, respectively. The band at  $3440\text{ cm}^{-1}$  is attributed to the OH functionality, while the  $1098\text{ cm}^{-1}$  band is due to asymmetric  $\text{C}-\text{O}-\text{C}$  stretching vibrations.

Due to significantly weaker water bands and minimized fluorescence Fourier transform Raman (FT-Raman) spectroscopy provide complementary information to FTIR measurements<sup>19,21</sup> and this method is particularly suited for water-soluble polymers. Figure 2 illustrates FT-Raman spectra of waterborne polyurethane (Trace A), polyester resin dispersion (Trace B), HDI isocyanurate (Trace C), and 2-methoxymethylethoxypropanol (Trace D). As shown in Figure 2, Traces A and B, asymmetric  $\text{C}=\text{C}-\text{CH}_2$  vibrational modes at  $3080\text{ cm}^{-1}$  are detected in polyurethane and polyester dispersions. The bands detected at  $2909$  and  $1124\text{ cm}^{-1}$  indicate the presence of  $\text{R}_3\text{C}-\text{H}$  and  $\text{C}-\text{C}$  stretching vibrations in isocyanurate (Trace C), and 2-methoxymethylethoxypropanol (Trace D). Figure 2, Trace D, confirms the presence of aldehyde in the additive, 2-methoxymethylethoxypropanol, detected at  $2829$  and  $2731\text{ cm}^{-1}$ .

As was shown in the previous studies,<sup>16,17</sup> crosslinking reactions leading to PUR formation can be quantified by following the decrease of the NCO band intensity at  $2271\text{ cm}^{-1}$  along with the increase of the  $\text{CO}_2$  (g) band at  $2337\text{ cm}^{-1}$ . The primary interest in following these species results from the fact that when NCO reacts with the active hydrogen of a hydroxy-functional compound, a urethane linkage is formed. This is illustrated in Scheme 1. However, in the presence of water, NCO can also react with  $\text{H}_2\text{O}$ . This is shown in Scheme 2.

When isocyanate reacts with water by condensation, an unstable intermediate, carbamic acid, is formed, which immediately dissociates to evolve carbon dioxide gas and an amine, which continues to react with free isocyanate to form urea. The NCO reaction with water can significantly affect film formation, as the evolution of carbon dioxide gas may result in unexpected property changes. Furthermore, vigorous reactions between isocyanates and amines may cause a rapid increase in molecular weight and viscosity, thus reducing pot life. Since amines are more nucleophilic than OH functional alcohols, urea reactions will occur faster and may predominate the crosslinking process. Under such circumstances, one could conclude that the presence of water is not desirable, especially that its presence may also result in hydrolysis of polyester linkages. However, inclusion of hydrophilic polyether tails surrounding NCO groups minimizes the influence of water and polyurethane formation dominates the process.<sup>23,24</sup>

Since we are interested in quantitative spectroscopic analysis of NCO and  $\text{CO}_2$ , it is necessary to obtain a calibration curve, where known concentrations of isocyanate and  $\text{CO}_2$  (g) are plotted against their respective band intensities. Using Beer-Lambert's law,

$$A = \epsilon b c \quad (2)$$

the molar absorption coefficient of isocyanate and  $\text{CO}_2$  (g) can be determined. Figure 3 represents the HDI isocyanurate and  $\text{CO}_2$  (g) band intensities at  $2271$  and  $2337\text{ cm}^{-1}$  plotted as a function of concentration. The slope of the calibration curve is the product of the path length and molar absorptivity, resulting in absorption coefficients of  $822.91\text{ l/mol}\cdot\text{cm}$  for NCO and  $168.36\text{ l/mol}\cdot\text{cm}$  for  $\text{CO}_2$  (g).<sup>17</sup> As crosslinking reactions progress, the isocyanate band intensity detected at  $2271\text{ cm}^{-1}$  de-

creases, while the band at  $2337\text{ cm}^{-1}$  attributed to  $\text{CO}_2$  gas formation increases.<sup>17</sup> The results presented in *Figure 4* show Circle ATR spectra recorded from 10 to 15 min.

As shown in *Scheme 2*, the presence of  $\text{CO}_2$  indicates reactions of water with isocyanate, and amine resulting from these reactions can further react with another free NCO to form urea. Using molar absorptivities determined in *Figure 3*, NCO and  $\text{CO}_2$  concentration changes were calculated at various stages of the reaction. This is illustrated in *Figure 5*. As seen, the NCO concentration decreases from  $3.93 \times 10^{-3}$  to  $2.48 \times 10^{-3}$  M, while the  $\text{CO}_2$  concentration increases from  $2.73 \times 10^{-3}$  to  $5.90 \times 10^{-3}$  M. During this time, from 10 to 50 min,  $\text{CO}_2$  increases approximately twice as fast as the decrease of NCO.

The amount of  $\text{CO}_2$  generated during polyurethane network formation is influenced by numerous factors, including the amount of water retained in the film at this stage of reaction, relative humidity (RH) of the environment as well as the amount of shear stresses imposed on the system. As shown in *Scheme 2*,  $\text{CO}_2$  is produced when NCO reacts with water. Increasing the amount of water or lowering evaporation rates enables water to be retained within the film, thus increasing the chance of  $\text{NCO-H}_2\text{O}$  reactions. Since higher relative humidity suppresses water evaporation, reactions shown in *Scheme 2* will be favorable. For the matter, higher shear rates imposed on waterborne PUR system may expose NCO particles to water, thus increasing the likelihood for reactions with water. To account for these features as well as in an effort to improve PUR chemical resistance, waterborne polyurethanes are formulated at 2:1 (NCO:OH) stoichiometry.<sup>25,26</sup>

In an effort to compare these results with the studies conducted on polyacrylate emulsions,<sup>17</sup> we formulated a polyester-based urethane at 1:1 NCO:OH and followed the decrease of NCO. *Figure 6* shows the NCO decrease for polyester and polyacrylate systems formulated at 1:1 stoichiometry and indicates that the rate of NCO consumption in the polyester system is greater, as determined from the slope of  $-9.53 \times 10^{-6}$  M/min. The slope for PUR acrylate is  $-3.05 \times 10^{-7}$  M/min, and this difference stems from the equivalent weight of the two waterborne systems. The acrylic emulsion has an equivalent weight of 3100 g/eq, whereas the polyester dispersion is approximately three times smaller, 1140 g/eq. Thus, when formulating the polyester dispersion as compared to the acrylic emulsion, the polyester requires more isocyanate at a given stoichiometry, which accelerates the crosslinking reactions leading to PUR network formation.

One would also expect that shear rates imposed on both 2K systems may affect the extent of reactions. After all, faster shear rates may expose NCO containing particles to  $\text{H}_2\text{O}$ , thus promoting reactions illustrated in *Scheme 2*. Therefore, shear requirements for these two waterborne systems should also be considered. Polyacrylate is an emulsion, while polyester is a dispersion, and this difference is reflected in viscosity behavior. The hydroxy-substituted polyacrylic emulsion exhibits a viscosity of 50-500 cps, whereas the polyester dispersion has a viscosity of 6000 cps. From an applica-

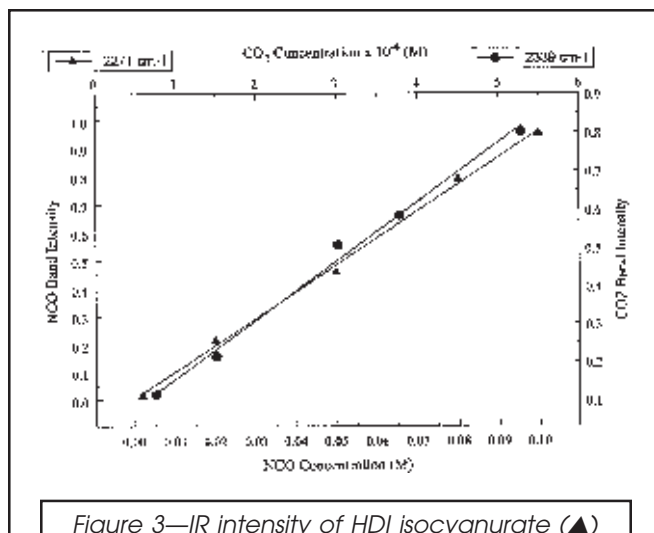


*Figure 3*—IR intensity of HDI isocyanurate ( $\blacktriangle$ ) and  $\text{CO}_2$  (g) ( $\bullet$ ) bands at  $2271$  and  $2337\text{ cm}^{-1}$  plotted as a function of concentration.

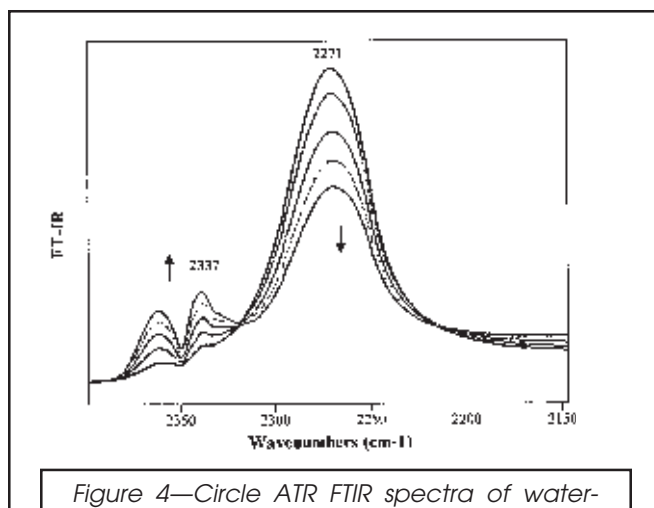


*Figure 4*—Circle ATR FTIR spectra of waterborne PUR recorded from 10 to 50 min in the  $2400\text{--}2200\text{ cm}^{-1}$  region.

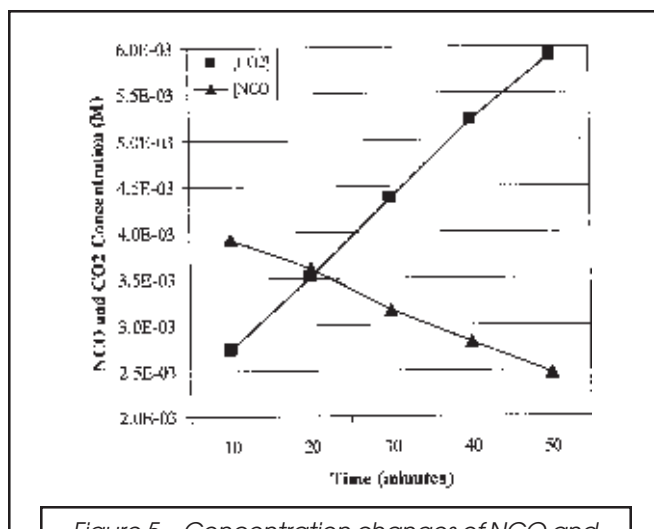


*Figure 5*—Concentration changes of NCO and  $\text{CO}_2$  species as a function of reaction time.

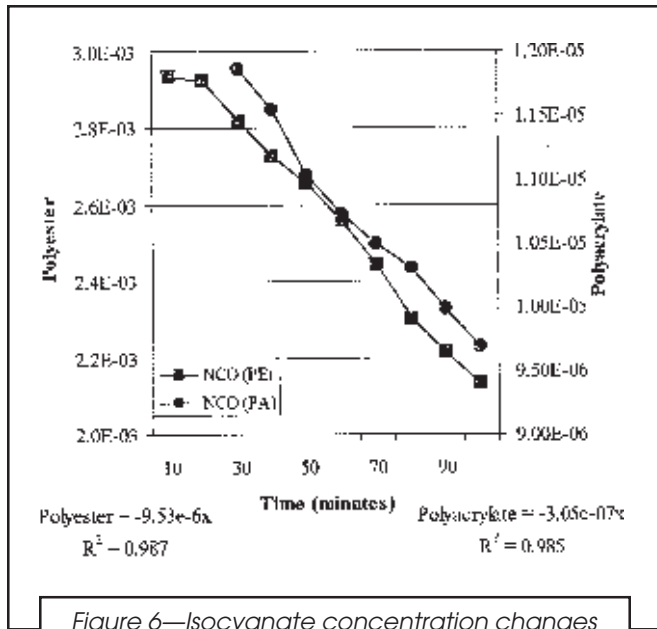


Figure 6—Isocyanate concentration changes resulting from crosslinking reactions in polyester (■) and polyacrylate (●) systems formulated at 1:1 (NCO:OH) ratio.

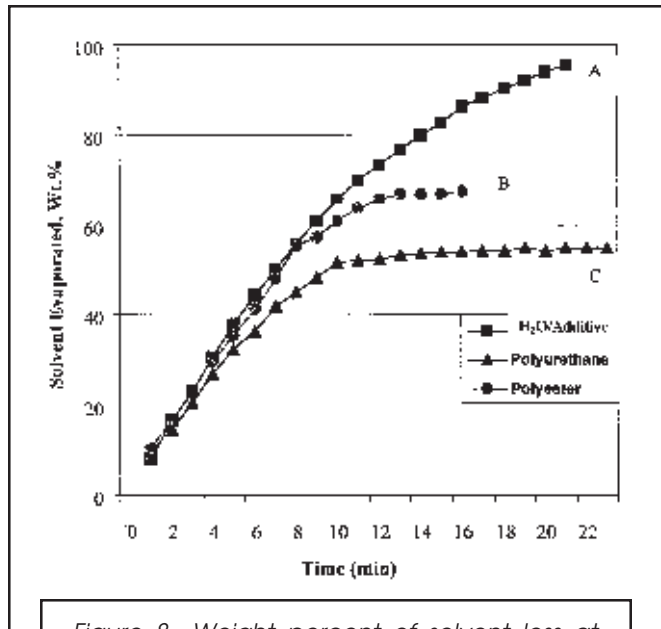


Figure 8—Weight percent of solvent loss at 20% RH of water/2-methoxymethylethoxypropanol (Trace A—■); polyester dispersion (Trace B—●); and formulated polyurethane (Trace C—▲).

tion point of view, this difference leads to different requirements for obtaining a uniform dispersion. The acrylic emulsion can be mixed with the polyisocyanate by creating a vortex with magnetic stirring bar, whereas the polyester dispersion requires a three-bladed propeller set at 48 rpm.

Previous studies have shown that shear rates may also affect particle sizes of isocyanate and polyol.<sup>23,24</sup> Because shears imposed on waterborne PUR may have an effect on the resulting chemical reactions and the amount of CO<sub>2</sub> gas evolved during urethane network formation, we conducted a series of experiments on polyester dispersions. The results are shown in Figure 7. As

shear forces increase, viscosity decreases, thus indicating shear thinning behavior attributed to structures of NCO-containing particles.<sup>27</sup> To disperse NCO in water, it is necessary to have hydrophilic polyether tails attached to the NCO-containing particle which act as a water barrier, minimizing reactions of NCO with water (Scheme 2). Such a structural feature allows the urethane crosslink to predominate over urea formation.

As these studies show, under high shear conditions, urethanes appear to give off more CO<sub>2</sub> gas, which comes from the reactions of NCO functionalities with H<sub>2</sub>O. This would indicate increased exposure of NCO to wa-

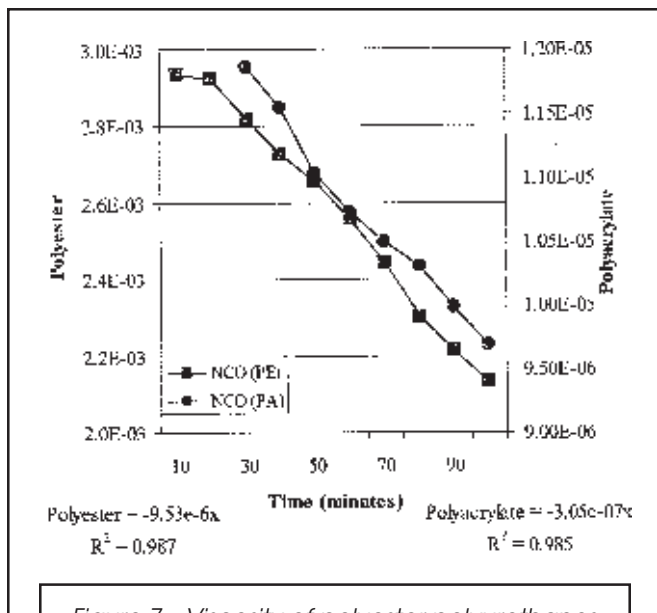


Figure 7—Viscosity of polyester polyurethanes vs. shearing rate in rpm.

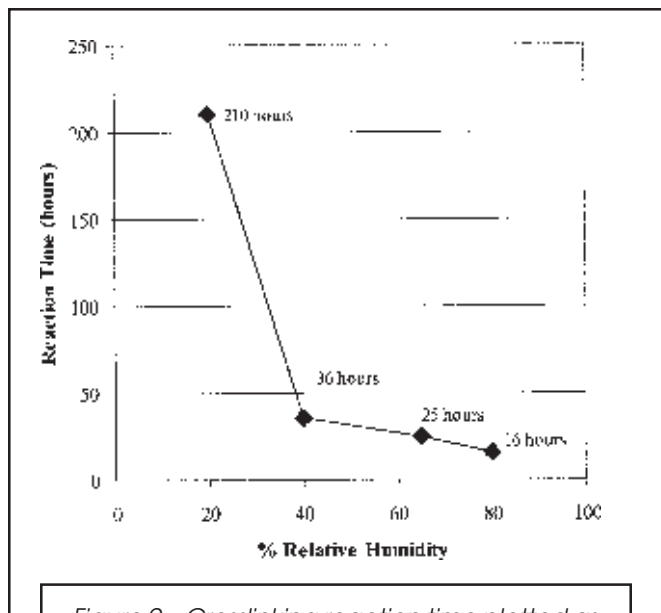


Figure 9—Crosslinking reaction time plotted as a function of relative humidity.

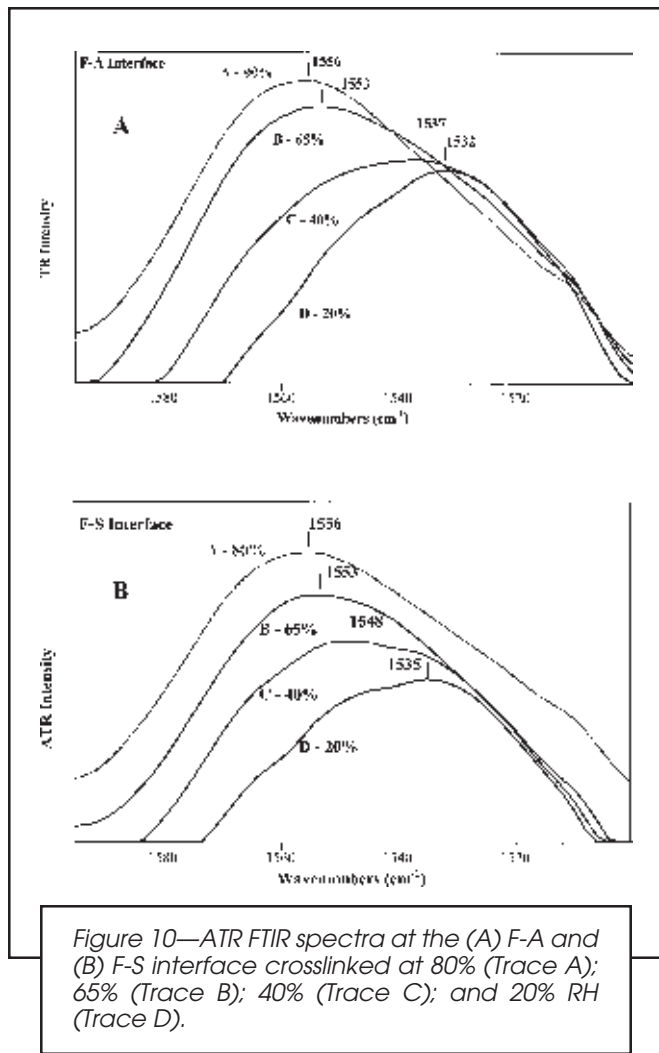


Figure 10—ATR FTIR spectra at the (A) F-A and (B) F-S interface crosslinked at 80% (Trace A); 65% (Trace B); 40% (Trace C); and 20% RH (Trace D).

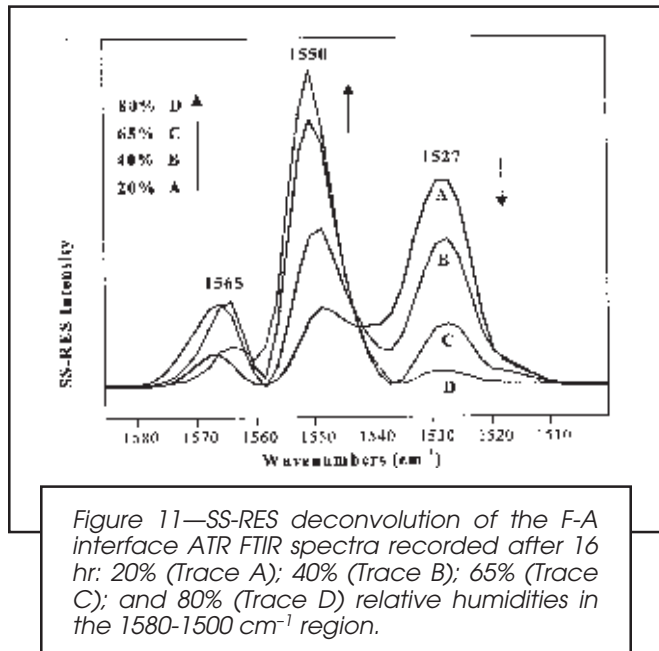


Figure 11—SS-RES deconvolution of the F-A interface ATR FTIR spectra recorded after 16 hr: 20% (Trace A); 40% (Trace B); 65% (Trace C); and 80% (Trace D) relative humidities in the 1580-1500 cm<sup>-1</sup> region.

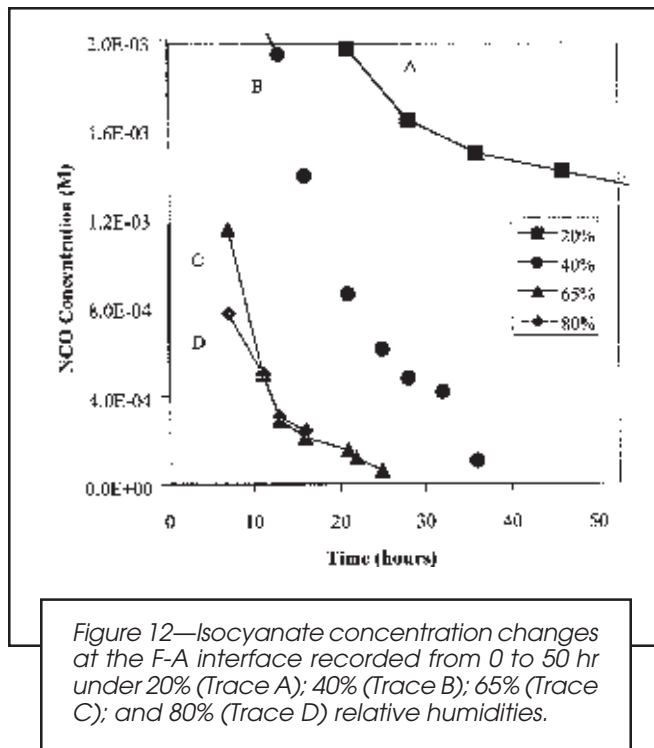


Figure 12—Isocyanate concentration changes at the F-A interface recorded from 0 to 50 hr under 20% (Trace A); 40% (Trace B); 65% (Trace C); and 80% (Trace D) relative humidities.

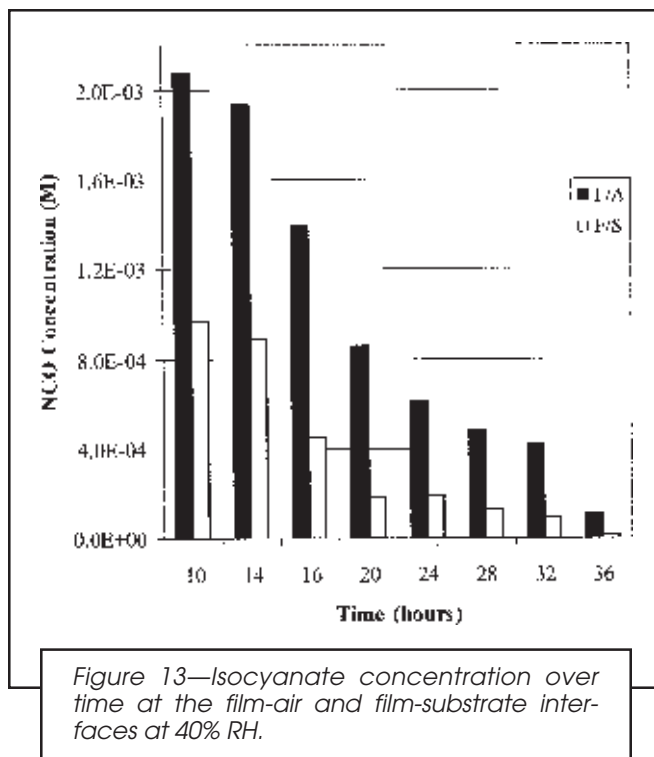


Figure 13—Isocyanate concentration over time at the film-air and film-substrate interfaces at 40% RH.

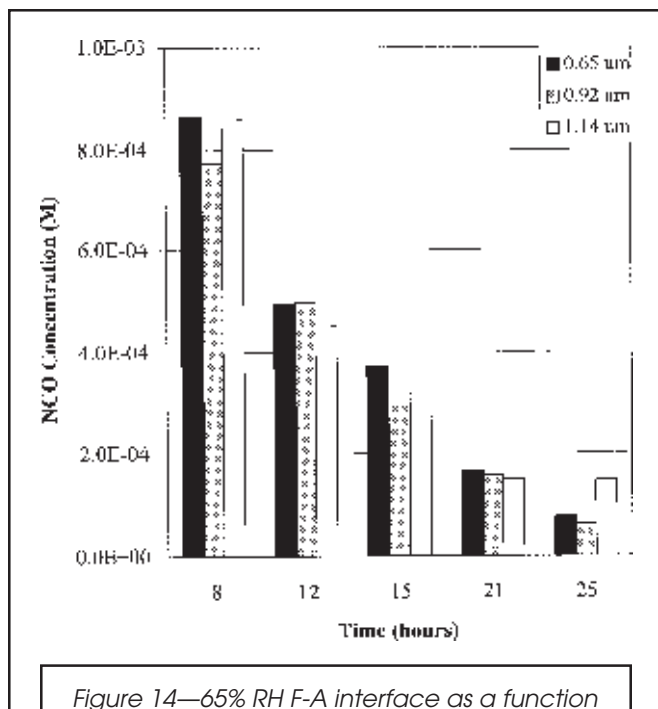


Figure 14—65% RH F-A interface as a function of distance from the surface.

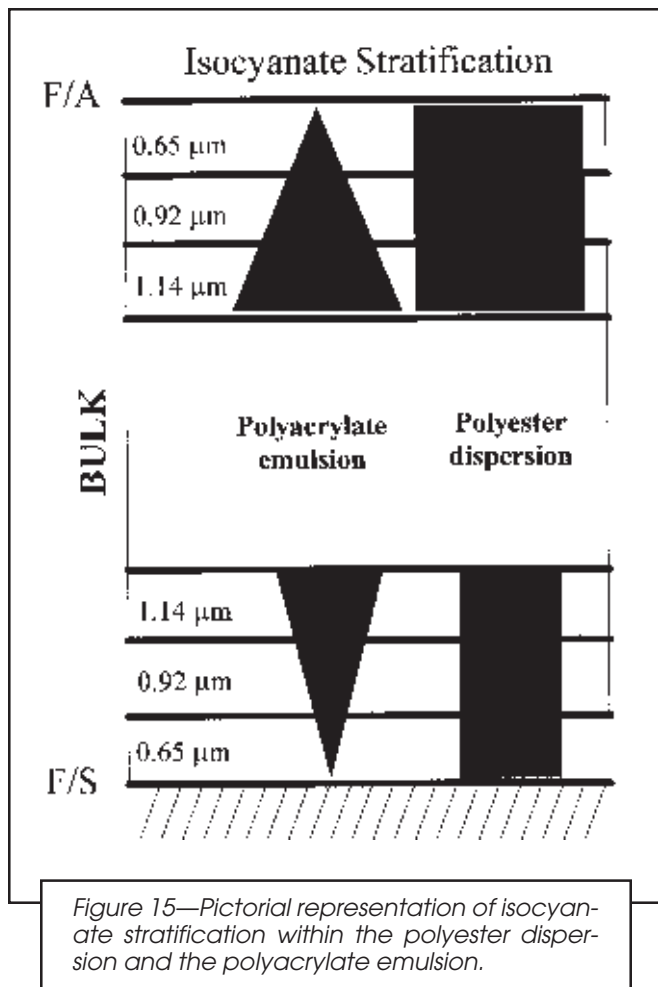


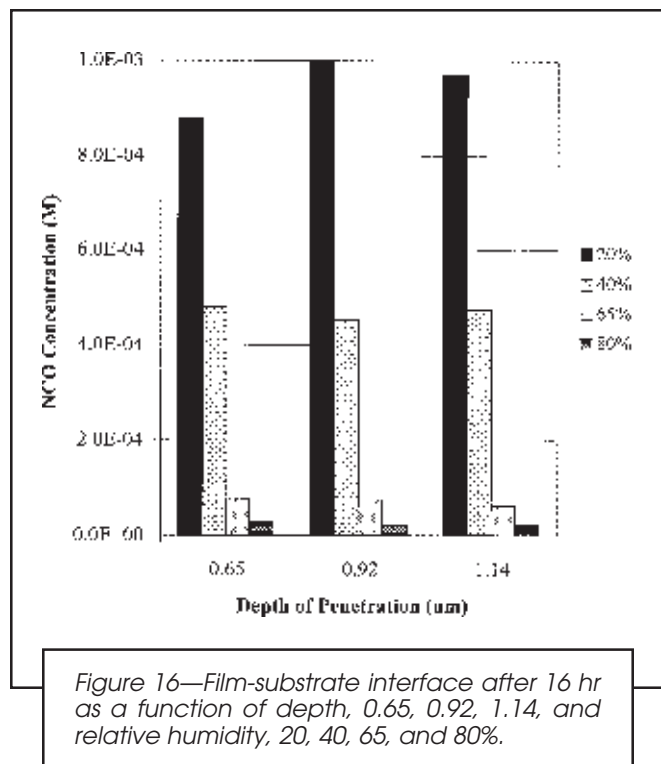
Figure 15—Pictorial representation of isocyanate stratification within the polyester dispersion and the polyacrylate emulsion.

ter and/or particle size changes as a result of shearing. The latter was suggested in previous studies.<sup>23,24</sup> Increased shear stresses induced on the NCO particle could either reorient or, under high shear, even remove hydrophilic polyether tails from the NCO-containing particles. Regardless of which process dominates, exposure of NCO particles increases the likelihood of reaction with water, thus increasing the amount of CO<sub>2</sub> gas given off.

Because the amount of water available for isocyanate reactions is critical, we examined how solvent evaporation rates affect chemical reactions. Figure 8 shows weight loss measurements of 2-methoxymethylethoxypropanol in DDI water (A), polyester dispersion (B), and waterborne PUR (C), plotted as a function of time at 25°C and 20% RH. These results show that during the first eight minutes, the rate of evaporation of 2-methoxymethylethoxypropanol:water (solvent), polyester oligomer, and PUR are the same, thus indicating that this stage is controlled by the partial vapor pressure of the system. After this period, the 2-methoxymethylethoxypropanol:water and polyester components continue to evaporate at a rapid rate, while PUR levels off at approximately 55% solids. The slope change indicates a transition from partial vapor pressure to diffusion-controlled evaporation, at which point approximately 10% of the original water concentration remains in the film for extended periods.

Because NCO functional groups can react with water available from the surrounding environment, relative humidity is expected to have a significant effect on the rate of isocyanate consumption. Figure 9 illustrates the effect of relative humidity on reaction times, where reaction times are equivalent to 100% isocyanate consumption. Because NCO is able to react with water contained in the film and also water vapor from the environment, the NCO consumption rate is highest at 80% RH after 16 hr of reaction. Reduction of relative humidity increases the time for NCO to be depleted within the first 1.14 μm from both F-A and F-S interfaces. For example, at 20% RH, it takes 210 hr for all NCO groups to be consumed. At low relative humidities, there are less pathways for the NCO to react, thus prolonging the crosslinking time. It should be remembered that in this study we examine the NCO changes that occur within the first 1.14 μm from the F-A and F-S interfaces. Consequently, NCO concentration levels of the bulk may be higher and thus inflate the crosslinking times presented in Figure 9.

As indicated earlier, ATR FTIR spectroscopy can easily detect urethane and polyurea formations. Both species exhibit overlapping bands due to the amide II stretching modes, which consist of NH bending and asymmetric stretching modes of CN. Using the maximum band intensity between the 1530-1560 cm<sup>-1</sup> region, the relative humidity influence on urethane and urea near the F-A and F-S interfaces was determined. This is illustrated in Figures 10A and B. Figure 10A shows how RH shifts the maximum of the 1532 cm<sup>-1</sup> band at 20% to 1556 cm<sup>-1</sup> at 80% RH. Similar behavior is observed at the F-S interface (Figure 10B). A shift of the amide II stretching mode reflects a transition from predominately urethane crosslinks at 20 and 40% RH to urea at 65 and 80% RH. Other studies have also detected urethane and urea vibrations at these wavenumbers.<sup>28,29</sup>



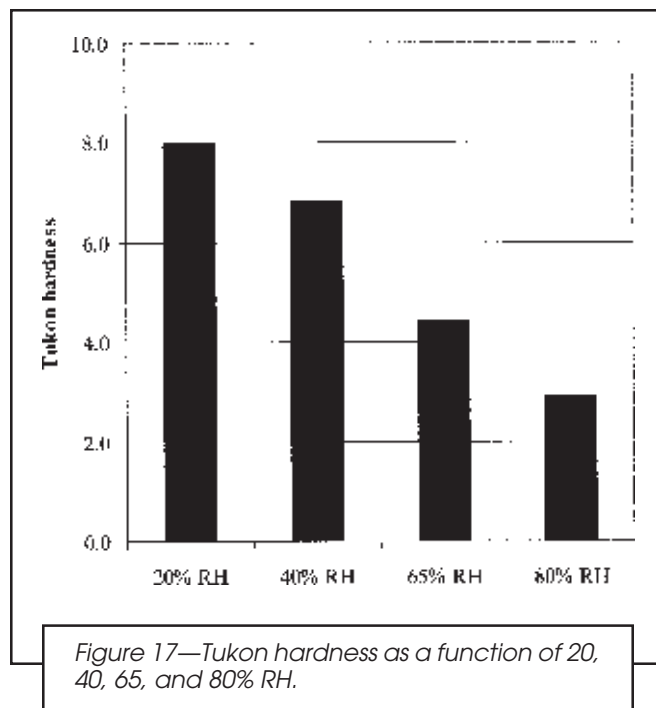
In an effort to determine relative amounts of polyurethane and polyurea, deconvolution using a maximum likelihood (ML) entropy approach was undertaken. Deconvoluted spectra were normally generated from the best estimation of a maximum probability approach using physical information about spectral features and statistical knowledge of the unknown number of overlapping bands. Figure 11 shows deconvolution of the 1580 to 1500  $\text{cm}^{-1}$  region at the F-A interface after 16 hr under 20, 40, 65, and 80% RH. As the RH increases from 20 to 80%, the band at 1527  $\text{cm}^{-1}$  decreases, while the 1550  $\text{cm}^{-1}$  band increases. While the band at 1550  $\text{cm}^{-1}$  is due to the amide II stretching modes of urea, the band at 1527  $\text{cm}^{-1}$  is attributed to the amide II stretching modes of urethane. These changes are attributed to the formation of urea at higher RHs, resulting from the NCO reaction with water. Because NCO groups react with water at higher relative humidity, reactions with OH functional groups of a resin are suppressed, thus a decrease of the 1527  $\text{cm}^{-1}$  band is observed.

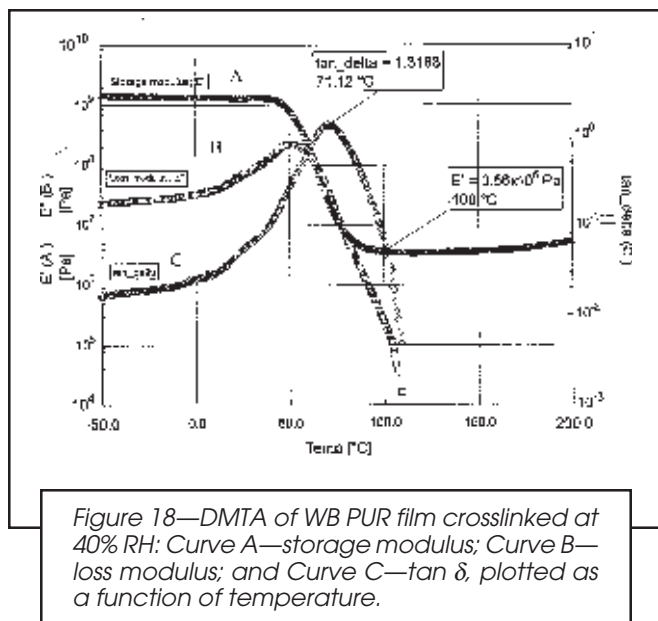
Because solvent evaporation and partial vapor pressure influence crosslinking reactions, the NCO concentration was monitored under 20, 40, 65, and 80% RH as a function of time, distance from the F-A and F-S interface, and polarization spectra were collected to examine possible orientation changes near the interfaces. Figure 12 illustrates the isocyanate concentration changes over time at the F-A interface under different relative humidities. Again, as shown in Figure 9, NCO reactions are accelerated at higher RHs and slow down at low RHs. For example, at 20% RH, only a 28% decrease of isocyanate concentration within 21 to 46 hr is observed. It should be noted that these data were not collected until a coherent film could be removed from the substrate, and 80% RH for seven hours was required. Thus, only a 68% change

in NCO concentration was detected. Since no changes in polarization experiments were detected, orientation of the functional groups is preferentially random.<sup>17</sup>

Because PURs are subjected to different external environments, NCO consumption at the F-A and F-S interfaces was examined. Figure 13 illustrates the differences in the NCO concentration at 40% RH. As shown, higher concentration levels of NCO are detected at the F-A interface. These results were obtained for all reaction times and agree with the data shown in Figure 10, where the intensity and wavenumber shifts for the amide II stretching modes are greater at the F-S interface, thus resulting in polyurea formation near the F-S interface. When the reactions are monitored between 10 to 36 hr at 40% RH, the NCO concentration difference between the F-A and F-S interfaces decreases from 47 to 9%. Previous studies concluded that the residual concentration of water present within the film enhances plasticization near the film-substrate interface, thus influencing isocyanate consumption.<sup>16,17</sup>

Isocyanate consumption as a function of depth within the film at the F-A and F-S interfaces was examined also. Depth of penetration studies can be performed using ATR FTIR spectroscopy by changing the angle of incidence light enters an ATR crystal.<sup>16,17,22</sup> Figure 14 summarizes the results of the depth profiling experiments conducted at the F-A interface under 65% RH. Again, as reactions progress, the NCO concentration decreases; and it appears that within the first few  $\mu\text{m}$  from the F-A interface, NCO remains constant. The same behavior was detected at the F-S interface, 0.65-1.14  $\mu\text{m}$ , although the degree of the NCO consumption was different. This behavior examined for the polyester dispersion appears to be different when compared to our previous polyacrylate emulsion studies,<sup>17</sup> where a strong dependence as a function of distance from the F-A and F-S interfaces was detected. Relative changes in isocyanate





concentration over time for the polyester dispersion and polyacrylate emulsion are summarized in Figure 15.

At this point it is appropriate to compare waterborne polyester and polyacrylate studies. Previous studies on polyacrylate emulsions revealed stratification within 0.65 to 1.14  $\mu\text{m}$  at both interfaces.<sup>17</sup> However, polyester dispersion does not exhibit this behavior and equivalent weight difference between polyester and acrylate, 1140 and 3100 g/eq, respectively, is attributed for this behavior. As was shown in Figure 6, the rate of the NCO reaction may determine whether stratification is observed on the monitored time scale. Because NCO is consumed faster for the polyester crosslinked PUR, stratification does not occur within the first few  $\mu\text{m}$  from F-A and F-S interfaces. On the other hand, slower reacting acrylate system stratification within 0.65 to 1.14  $\mu\text{m}$  at both interfaces is detected.

Figure 16 illustrates the changes in isocyanate concentration as a function of depth and RH after 16 hr of crosslinking. After 16 hr, NCO concentration levels at 40% RH are approximately 51% of the NCO concentration at 20% RH. As shown in Figure 16, the distance from the substrate has no effect on the NCO concentration as a function of RH for the polyester dispersion. All changes observed in Figures 14 and 16 are within the standard deviation for each sample.

Knowing the relative humidity, water retained in the film, and shear rates influence crosslinking reactions of

Table 2— $T_g$  and XLD of WB PUR Film Crosslinked at 20, 40, 65, and 80% RH

WB-PUR film crosslinked at:	$T_g$ (°C)	Crosslink Density XLD (mol/cm <sup>3</sup> ) (calculated at 100°C)
20% RH	70.8	$5.2 \times 10^{-4}$
40% RH	71.1	$3.8 \times 10^{-4}$
65% RH	68.2	$3.1 \times 10^{-4}$
80% RH	68.1	$1.8 \times 10^{-4}$

WB PURs, it is appropriate to correlate structure-property relationships for PURs crosslinked at 20, 40, 65, and 80% RH. Conical mandrel flexibility (ASTM D 522) and reverse impact resistance (ASTM D 2794) show no changes as a function of RH, having the highest flexibility and reverse impact resistance at 1/8 in. and 110 in.-lb, respectively. However, as illustrated in Figure 17, Tukon hardness reveals the effect of RH. As RH increases, the Tukon hardness decreases from 8 to 2.9, which is attributed to polyurea formation.

Because relative humidity induced structural changes of the WB PUR, dynamic mechanical thermal analysis (DMTA) was conducted.<sup>30</sup> The results of DMTA analysis are illustrated in Figure 18 for a PUR specimen crosslinked at 40% RH. As seen, the maximum of the tan  $\delta$  peak at 71°C is the glass transition temperature ( $T_g$ ), and using the storage modulus minimum in the rubbery plateau region at 100°C, the XLD was calculated as  $3.8 \times 10^{-4}$  mol/cm<sup>3</sup>. Table 2 summarizes the  $T_g$  and XLD recorded for WB PUR films crosslinked at 20, 40, 65, and 80% RH. As expected, higher RH results in lower XLD, which is also reflected in hardness as well as molecular level spectroscopic measurements.

## CONCLUSIONS

Factors that influence waterborne polyurethane film formation were examined using ATR FTIR spectroscopy at the F-A and F-S interfaces and correlated to macroscopic measurements. These studies show that polyurethane and polyurea are detected and relative humidity significantly influences the time and type of crosslinking reactions. NCO content at the F-A interface is higher than the F-S interface, and the depth profiling experiments from 0.65 to 1.14  $\mu\text{m}$  reveal no stratification of NCO. However, increased polyurea content at deeper depths from both interfaces are detected. Solvent evaporation experiments showed a solvent evaporation-controlled stage within the first eight minutes of reaction time at 20% RH. After this period, the process is diffusion controlled, where approximately 10% of the original concentration of water remains in the film for extended periods.

WB PUR exhibits shear thinning behavior and increased shear rates generate higher CO<sub>2</sub> contents during the film formation, ultimately leading to a viscosity decrease. These data suggest that NCO particles have a greater tendency for interactions with water under high shear rates. A comparison of polyester dispersion and polyacrylate emulsion polyurethanes shows different stratification profiles of the NCO. While polyester urethane consumes NCO faster due to differences in equivalent weight, this process may diminish stratification processes observed for slower reacting polyacrylate polyurethanes. Relative humidity also has an influence on macroscopic properties. Although no differences were detected for flexibility and reverse impact resistance tests, most likely due poor sensitivity of these measurements, Tukon hardness decreased for PUR films crosslinked at higher RHs. These results agree with DMTA data, which showed that for films crosslinked at higher RH, the  $T_g$  and XLD are lower due to polyurea formation. Since it is

apparent that urethane film formation is sensitive to environmental effects, our future studies will involve the effect of substrates on their film formation.<sup>31</sup>

## ACKNOWLEDGMENTS

The authors acknowledge the National Science Foundation Industry/University Cooperative Research Center in Coatings at North Dakota State University and Eastern Michigan University as well as the Bayer Corporation for funding these studies.

## References

- (1) Jacobs, P.B. and Yu, P.C., "Two-Component Waterborne Polyurethane Coatings," *JOURNAL OF COATINGS TECHNOLOGY*, 64, No. 820, 45 (1993).
- (2) Blank, W.J. and Tramontano, V.J., *Prog. Org. Coat.*, 27, 1 (1996).
- (3) Tramontano, V.J. and Blank W.J., "Crosslinking of Waterborne Polyurethane Dispersions," *JOURNAL OF COATINGS TECHNOLOGY*, 67, No. 848, 89 (1995).
- (4) Rosthauser, J.W. and Nachtkamp, K., *Advances in Urethane Science Technology*, Technomic, Westport, CT, Vol. 10, 121-162, 1987.
- (5) Padget, J.C., "Polymers for Water-Based Coatings—A Systematic Overview," *JOURNAL OF COATINGS TECHNOLOGY*, 66, No. 839, 89 (1994).
- (6) Satguru, R., McMahon, J., Padget, J.C., and Coogan, R.G., "Aqueous Polyurethanes—Polymer Colloids with Unusual Colloidal, Morphological, and Application Characteristics," *JOURNAL OF COATINGS TECHNOLOGY*, 66, No. 830, 47 (1994).
- (7) Dieterich, D., *Prog. Org. Coat.*, 9, 281 (1981).
- (8) Kahl, L. and Bock, M., "Waterborne Two-Component PU Clear Coats for Automotive Coatings: Development of Raw Materials and Mixing Technology," *Proc. Third Nurnburg Congress*, Nurnburg, Germany, March 13-15, 1995.
- (9) Jacobs, P.B. and McClurg, D.C., "Water-Reducible Polyurethane Coatings for Aerospace Applications," *Proc. Low and No VOC Coating EPA Conference*, San Diego, CA, May 25-27, 1993.
- (10) Bittner, A. and Ziegler, P., "Waterborne Two-Pack Polyurethane Coatings for Industrial Applications," *Proc. Third Nurnburg Congress*, Nurnburg, Germany, March 13-15, 1995.
- (11) Renk, C.A. and Swartz, A.J., "Fast Drying, Ultra Low VOC, Two-Component Waterborne Polyurethane Coatings for the Wood Industry," *Proc. 22nd Waterborne, High-Solids, and Powder Coatings Symposium*, New Orleans, LA, February 22-24, 1995.
- (12) Bock, M. and Petzoldt, "Aqueous Polyurethane Coating Systems for Plastics," *Proc. 22nd Waterborne, High-Solids, and Powder Coatings Symposium*, New Orleans, LA, February 22-24, 1995.
- (13) Francois, P., Vaudaux, P., Nurdin, N., Mathieu, H.J., and Descousts, P., *Biomaterials*, 17, 667 (1996).
- (14) Dearth, R.S., Mertes, H., and Jacobs, P.J., *Prog. Org. Coat.*, 29, 73 (1996).
- (15) Lee, H.T., Hwang, Y.T., Chang, N.S., Huang, C.T., and Li, H.C., "Structure-Property Relationships of Aqueous Polyurethane Dispersions," *Proc. 22nd Waterborne, High-Solids, and Powder Coatings Symposium*, New Orleans, LA, February 22-24, 1995.
- (16) Kaminski, A.M. and Urban, M.W., "Interfacial Studies of Crosslinked Polyurethanes: Part I. Quantitative and Structural Aspects of Crosslinking Near Film-Air and Film-Substrate Interfaces in Solvenborne Polyurethanes," *JOURNAL OF COATINGS TECHNOLOGY*, 69, No. 872, 55 (1997).
- (17) Kaminski, A.M. and Urban, M.W., "Interfacial Studies of Crosslinked Urethanes: Part II. The Effect of Humidity on Waterborne Polyurethanes, A Spectroscopic Study," *JOURNAL OF COATINGS TECHNOLOGY*, 69, No. 873, 113 (1997).
- (18) Urban, M.W., *Attenuated Total Reflectance Spectroscopy of Polymers; Theory and Practice*, American Chemical Society, Washington, D.C., 1996.
- (19) Urban, M.W., *Vibrational Spectroscopy of Molecules and Macromolecules on Surfaces*, Wiley, New York, 1993.
- (20) Storer, R., *1990 Annual Book of ASTM Standards*, Section 6—Paints, Related Coatings & Aromatics, Vol. 1, 2, 3, Easton, MD, ASTM, 1990.
- (21) Urban, M.W. and Craver, C.D. (Eds.), *Structure-Property Relations in Polymers*, American Chemical Society, Washington, D.C., 1993.
- (22) Ludwig, B.W. and Urban, M.W., "Effect of Polyurethane Curing Conditions on the Delamination of Pressure Sensitive Films," *JOURNAL OF COATINGS TECHNOLOGY*, 66, No. 839, 59 (1994).
- (23) Dvorchak, M.J., "Using High Performance Two-Component Waterborne Polyurethane Wood Coatings," *JOURNAL OF COATINGS TECHNOLOGY*, 69, No. 866, 47 (1997).
- (24) Bui, H., Dvorchak, M., Hudson, K., and Hunter, J., *European Coatings J.*, 5, 476 (1997).
- (25) Rohm and Haas Technical Brochure, "Two-Component Waterborne Polyurethane Wood Coatings," Philadelphia, PA, 1995.
- (26) Wicks, Z. Jr., Jones, F., and Pappas, S., *Organic Coatings Science and Technology*, Vol. 1, Wiley, New York, 1992.
- (27) Bui, H., Dvorchak, M., Hudson, K., and Hunter, J., *European Coatings J.*, 5, 476-481 (1997).
- (28) Khranovskii, V.A. and Gul'ko, L.P., *J. Macromol. Sci.-Phys.*, 22, 497 (1983).
- (29) Ishihara, H., Kimura, K., Saito, K., and Ono, H., *J. Macromol. Sci.-Phys.*, 10, 591 (1974).
- (30) Hill, L. and Kozlowski, K., "Crosslink Density of High-Solids MF-Cured Coatings," *JOURNAL OF COATINGS TECHNOLOGY*, 59, No. 751, 63 (1987).
- (31) Urban, M.W., et al., *JOURNAL OF COATINGS TECHNOLOGY*, submitted 1998.